

## **NUMERICAL ANALYSIS OF OUT-OF-PLANE LOADED MASONRY WALL USING HOMOGENIZATION TECHNIQUE**

S. YU, C. WU, M.C. GRIFFITH

School of Civil and Environmental Engineering  
The University of Adelaide, SA, Australia

### **SUMMARY**

The homogenization technique has been used in the past to derive the equivalent material properties and failure characteristics for solid brick masonry and recently it has been employed to investigate the complex mechanical properties of hollow concrete block masonry. However, few studies have been carried out to derive the equivalent material properties of standard ten-core brick masonry in Australia. In this paper, a very detailed finite element model is used to model a three-dimensional basic cell to derive the equivalent material properties for a homogenous masonry unit. Various load cases are applied on the basic cell surfaces to derive average stress-strain relationships of the homogenous masonry unit under different stress states. The average elastic properties and failure characteristics of the homogenous masonry unit are obtained from the simulated results. The numerical results are verified by comparing to experimental results from previous tests at the University of Adelaide and numerical results from simulation using a distinct finite element model. The derived equivalent material properties can be utilized to simulate large-scale masonry structures and predict their failure modes under out-of plane loading.

### **BACKGROUND**

Considerable research has been conducted to investigate the complex mechanical behavior of solid brick masonry structures using various theoretical and numerical homogenization techniques in the last decade (Anthoine 1995; Luciano and Sacco 1997; Ma et al. 2001; Zucchini and Lourenco 2002; Zucchini and Lourenco 2004; Milani et al. 2006). It has been shown that using homogenized material properties can give a reliable estimation of masonry response under both static and dynamic loading, however, substantially less computational time is taken to perform the analysis of masonry structures as compared with distinctive model in which bricks and mortar joints are separately discretized. Recently, the homogenization technique has been used to derive equivalent material properties of hollow concrete block masonry (Wu and Hao 2007). However, no study has been conducted to analyse the response of masonry structure constituted by ten-core brick units jointed with mortar using the homogenization technique. Due to the complex geometric properties of the ten-core brick unit, it is very complicated and time consuming to use the distinctive model to perform the analysis of this kind of masonry structures. Therefore it is of importance if the equivalent material properties of this masonry structure can be derived.

In this paper, a basic cell is numerically modelled to derive the equivalent material properties and failure characteristics of masonry unit. In the numerical model, the basic cell is modelled with distinctive consideration of individual components of mortar and ten-core brick units. Drucker-Prager strength theory is used for both mortar and brick. The average stress-strain relationships of the basic cell under different stress states are derived by applying various displacement boundaries on the basic cell surfaces. The equivalent material properties and failure characteristics of masonry material are derived from the simulation results. The developed homogenized model is validated in analysis of the response of a masonry wall subjected to out-of-plane loads.

## HOMOGENIZATION PROCESS

Masonry is a composite structure constituted by bricks and mortar. Traditionally laboratory tests are performed to get the average stress and strain relationships of a specimen in order to obtain the homogenized properties of composite materials such as concrete with aggregates and cement. For masonry structures, it is difficult to conduct the laboratory test. Therefore, the numerical homogenization method is used in this study to derive its equivalent material properties. Figure 1 shows the homogenization process for a basic cell which contains all the geometric and constitutive information of the masonry wall. The basic cell is modelled, separately, with individual components of mortar and brick. Constitutive relations of the basic cell can be set up in terms of average stresses and strains from the geometry and constitutive relationships of the individual components. The average stress and strain  $\bar{\sigma}_{ij}$  and  $\bar{\varepsilon}_{ij}$  are defined by the integral over the basic cell as

$$\bar{\sigma}_{ij} = \frac{1}{V} \int_V \sigma_{ij} dV \quad (1)$$

$$\bar{\varepsilon}_{ij} = \frac{1}{V} \int_V \varepsilon_{ij} dV \quad (2)$$

where  $V$  is the volume of the basic cell,  $\sigma_{ij}$  and  $\varepsilon_{ij}$  are stress and strain components in an element. By applying various displacement boundary conditions on the surfaces of the basic cell, the equivalent stress-strain relationships of the basic cell are established and the equivalent material properties of the basic cell can be derived from the simulated stress-strain curves.

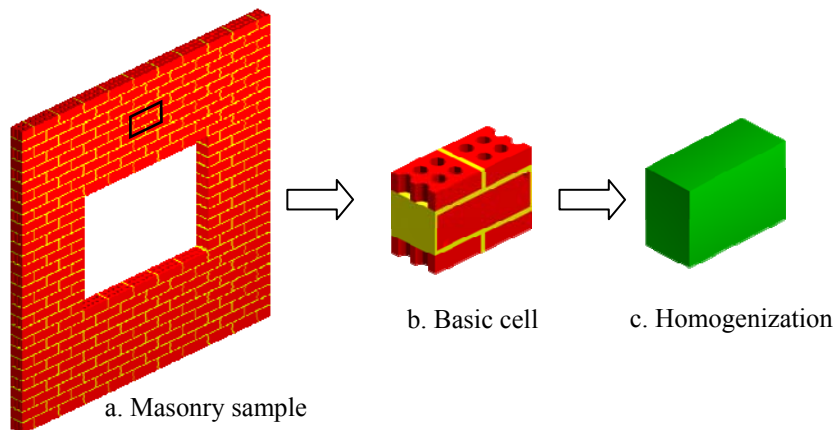


Figure 1 Homogenization of masonry material

## MATERIAL MODELS FOR BRICK AND MORTAR

In order to derive the equivalent inelastic material properties of the basic cell, reliable material models for brick and mortar are important. The yield criterion for quasi-brittle materials such as brick and mortar is usually based on Drucker-Prager strength theory. The Drucker-Prager yield condition is given by:

$$\alpha I_1 + \sqrt{J_2} - k = 0 \quad (3)$$

where  $J_2$  is the second invariant of the deviatoric stress tensor  $S_{ij}$ ,  $I_1$  is the first invariant of the stress tensor, given by  $J_2 = 0.5s_{ij}s_{ij}$ ,  $I_1 = (\sigma_1 + \sigma_2 + \sigma_3)$ .  $\alpha$  is the pressure sensitivity coefficient and  $k$  is a material constant.

Typical 10-core clay brick unit manufactured by Hallet Brick Ptd Ltd with nominal dimensions of  $230 \times 110 \times 76$  mm<sup>3</sup> as shown in Figure 2 is used in this study. The detail dimensions and locations of 10 cores are also shown in Figure 2. The mortar consisted of cement, lime and sand mixed in the proportions of 1:2:9. This 10-core clay brick unit and a 10 mm thick mortar joint are used in this study. In the analysis, the same material properties for bed and head joints are assumed. Table 1 lists material properties for mortar and brick. Details about the masonry properties are presented elsewhere (Griffith and Vaculik 2007). The above Drucker-Prager strength model and material properties for brick and mortar is coded into a finite element program LSDYNA to calculate the stress-strain relationships of the basic cell as shown in Figure 1b.

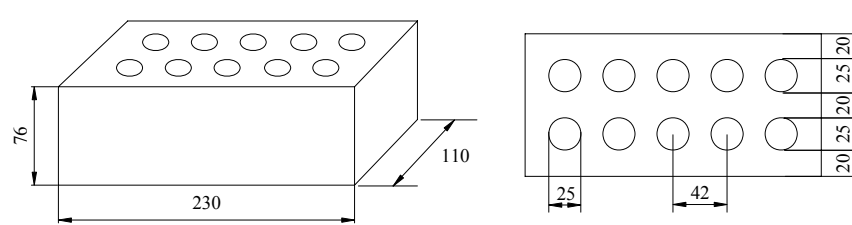


Figure 2 Nominal dimensions of brick unit (mm)

Table 1 Material properties for brick and mortar

	$E_c, E_t$ (GPa)	$G_c$ (GPa)	$\nu$	$\sigma_t$ (MPa)	$\sigma_c$ (MPa)	$\alpha$	$K$ (MPa)
brick	5.27	2.2	0.2	3.55	35.5	0.47	3.73
mortar	0.44	0.18	0.3	0.6	6.14	0.47	0.65

## CONVERGENCE TESTS ON THE BASIC CELL

The finite element mesh used in the numerical model of the basic cell is shown in Figure 3. As shown, the 10-core clay brick unit and mortar in the basic cell are discretized into a number of solid elements. Before the numerical analysis, convergence test on the influence of element size on computational accuracy is carried out by halving the size of the element for both brick and mortar while keeping loads on the basic cell unchanged until the difference between the results obtained with two consecutive element sizes is less than 5%. Totally, 3560 eight-node solid elements are used in the numerical model of the basic cell to achieve the reliable estimation. The final numerical model used in the simulation is shown in Figure 3. By applying various

displacement boundary conditions, a complete monotonic stress-strain relation can be derived through the homogenization process.

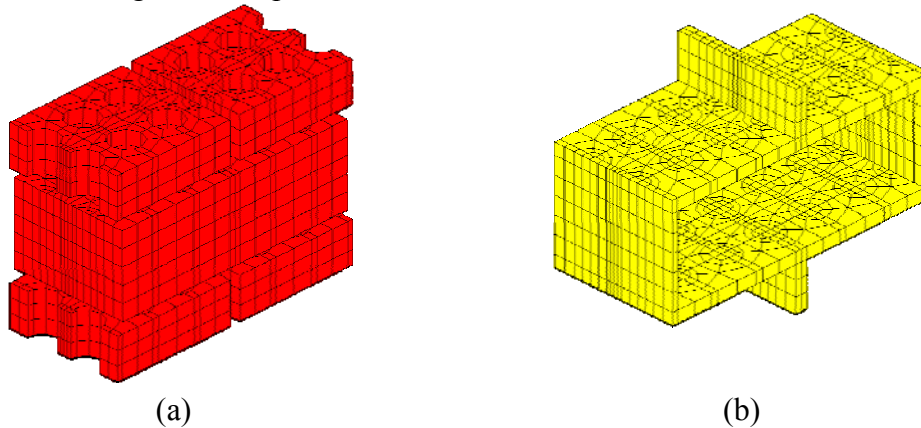


Figure 3 Masonry Basic Cell Finite Element Model: (a) brick, (b) mortar

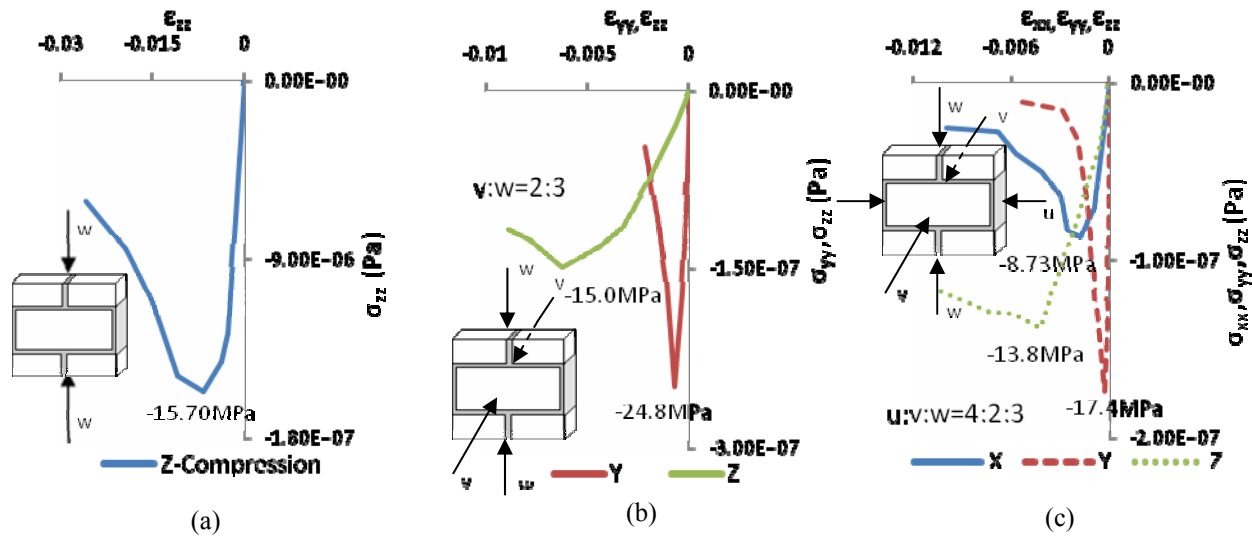
### **SIMULATED STRESS-STRAIN RELATIONSHIPS OF THE BASIC CELL**

The response of the basic cell under compressive-compressive, compressive-tensile, tensile-tensile, compressive-shear and tensile-shear stress states are simulated in this study. Figure 4 shows the typical stress-strain curves of the basic cell under uniaxial compressive-compressive stress states. As shown in Figure 4a, the uniaxial compressive strength in Z direction is 15.7 MPa, which is quite close to the experimental result of ultimate masonry compressive strength 16.0 MPa carried out by Griffith and Vaculik (2007). It shows that the uniaxial compressive strengths of the basic cell in X and Y directions are 7.88 MPa and 7.39 MPa from the simulation results of uniaxial compressive-compressive states in X and Y directions, respectively, indicating that the geometry of hollow bricks with ten cores reduces the compressive strength of the basic cell in both X and Y directions significantly.

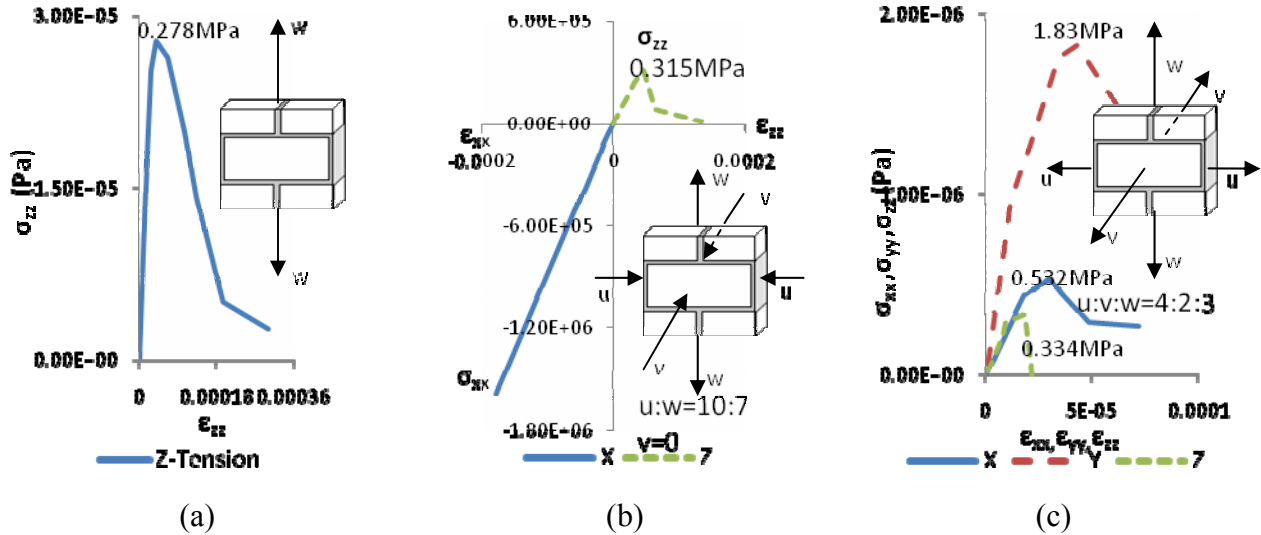
As the basic cell under biaxial or triaxial compressive states, its strength enhancement in Z direction is not observed although there are significant strength enhancement in X and Y direction. When the basic cell is under biaxial compressive loads in Y and Z directions as shown in Figure 4b, its maximum compressive strength in Z direction is 15.0 MPa, slightly smaller than its uniaxial strength although the maximum strength in Y direction is 24.8 MPa, much higher than its uniaxial compressive strength. It also shows in Figure 4c that the maximum compressive strengths of the basic cell under triaxial compressive states in X, Y and Z directions are 8.73, 17.4 and 13.8 MPa, respectively, and the compressive strength in Z direction is also slightly smaller than its uniaxial compressive strength. It should be noted that due to different dimensions of the basic cell in X, Y and Z directions, the ratios of the displacement in Y and Z directions as shown in Figure 4b and in X, Y and Z directions as shown in Figure 4c are set to be 2:3 (v:w) and 4:2:3 (u:v:w) according to the dimension of the representative element so that the strain ratios in Y and Z directions and in X, Y and Z directions is about 1:1 and 1:1:1.

Fig. 5 shows the typical stress-strain curves in compressive-tensile and tensile-tensile stress states. The uniaxial tensile strengths in X, Y and Z directions are 0.85 MPa, 1.84 MPa and 0.28 MPa. It can be seen that the tensile strength of the basic cell in Z direction is much smaller than tensile strength of mortar (0.6 MPa) because the volume of the cores is counted as part of the total volume of the basic cell as well as geometric size influence. The simulated results also indicate that there is not a significant tensile strength enhancement in Z direction when the basic cell is

under biaxial or triaxial tensile stress states. Under tensile-compressive stress state, the ultimate tensile strength slight increases. It can be observed from Figure 5b that the basic cell fails owing to tensile strain before the compressive strength reaches to the maximum value. When the basic cell under triaxial tensile states (see Figure 5c), its tensile strengths in X and Y direction reduce although there is a slight increase in its tensile strength in Z direction.



**Figure 4** Typical stress-strain relationships of basic cell in compressive-compressive stress states.



**Figure 5** Typical stress-strain relationships of the basic cell in compressive-tension stress state.

The representative stress-strain curves of the basic cell under the compressive-shear and tensile-shear stress state is shown in Figure 6. The ultimate shear strengths  $\tau_{zx}$ ,  $\tau_{zy}$  and  $\tau_{yx}$  under pure shear condition are 0.78 MPa, 1.58 MPa and 1.28 MPa, respectively. It also shows in Figure 6b that under compressive-shear stress state, the basic cell fails due to shear strain before the compressive strength reaches the maximum value.

Based on the simulated stress-strain curves, the equivalent material properties of the basic cell such as Young's moduli, shear moduli and Poisson's ratio as listed in Table 2 are derived.

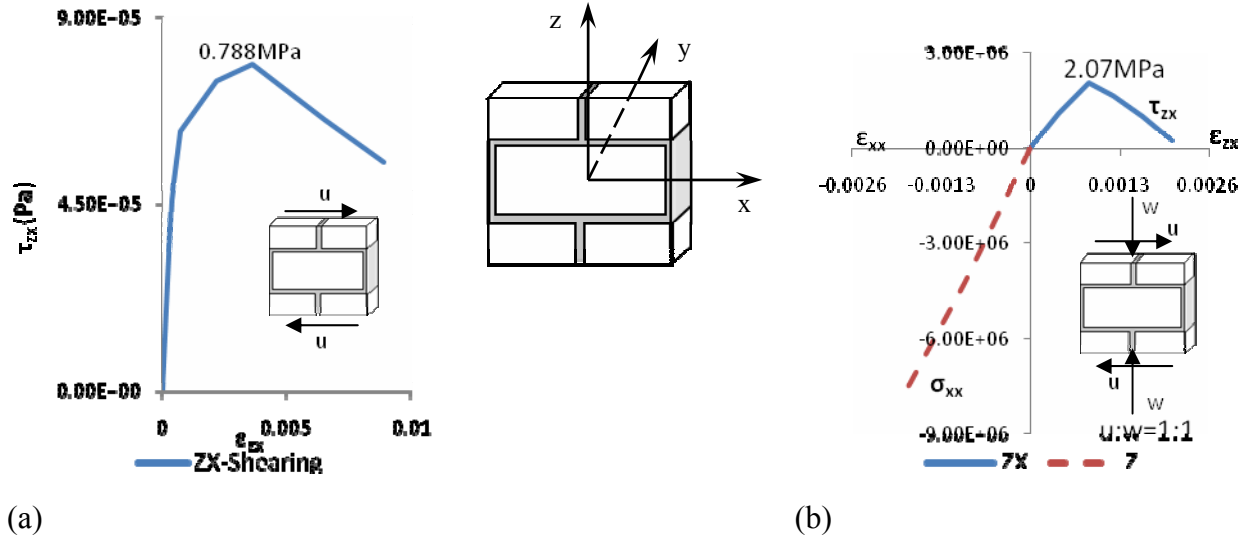


**Figure 6** Stress-strain relationships of the basic cell in shear stress state.

Table 2 Equivalent material properties for masonry unit

Young's Modulus / Pa			Shear Modulus / Pa			Poisson's Ratio		
$E_{xx}$	$E_{yy}$	$E_{zz}$	$G_{xy}$	$G_{yz}$	$G_{zx}$	xy	yz	zx
7.49E+09	4.82E+10	6.82E+09	7.35E+09	2.33E+09	1.28E+09	0.250	0.269	0.205

## DEVELOPMENT OF FAILURE CRITERIA

The equivalent strength envelope for ten-core brick masonry can be derived using the ultimate strength from the simulated stress-strain curves. Since the masonry is an orthotropic material, conventional strength criteria such as the Drucker-Prager or Mohr-Coulomb strength criterion, are not suitable for representing the strength envelope of the orthotropic basic cell. The observations demonstrate that there is little strength enhancement in Z direction and therefore the failure criteria in Z direction follows maximum normal stress criteria for both tensile and compressive strength. In XY plane its failure surface of the basic cell is shown in Figure 7. Therefore, the failure criteria are represented by tensile and compressive failure in Z direction

$$\sigma_{zz} = X_c \quad (4)$$

$$\sigma_{zz} = X_t \quad (5)$$

Tensile and compressive failure in XY plane

$$\frac{1}{Y_t}(\sigma_{xx} + \sigma_{yy})^2 + \frac{\tau_{xy}^2 - \sigma_{xx}\sigma_{yy}}{S_c^2} = 1 \quad (6)$$

$$\frac{1}{Y_c} \left[ \left( \frac{Y_c}{2S_c} \right)^2 - 1 \right] (\sigma_{xx} + \sigma_{yy}) + \frac{1}{4S_c^2} (\sigma_{xx} + \sigma_{yy})^2 - \frac{(\tau_{xy}^2 - \sigma_{xx}\sigma_{yy})}{S_c^2} = 1 \quad (7)$$

where  $X_T$  and  $X_C$  are the tensile strength and compressive strength in Z direction;  $Y_T$  and  $Y_C$  are average tensile and compressive strength in X and Y directions;  $S_C$  is shear strength in XY plane. . Using the simulated data, it is found that  $X_T = 0.28$  MPa,  $X_C = 15.7$  MPa,  $Y_T = 1.35$  MPa,  $Y_C = 7.65$  MPa. To simplify the matters, the failure criteria in XY plane is expressed in term of the principle stresses in XY plane,  $\sigma_1$  and  $\sigma_2$ , which are derived from  $\sigma_X$ ,  $\sigma_Y$  and  $\tau_{XY}$  in plane stress system.

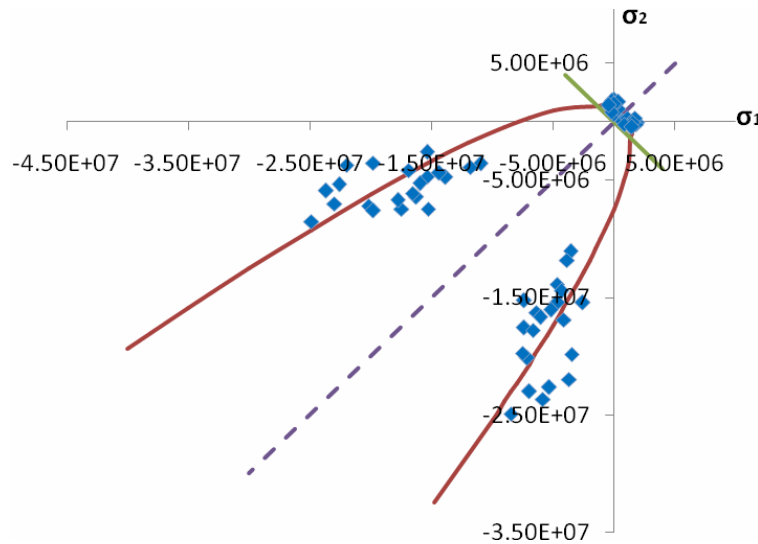


Figure 7 Failure curve in XY plane

## VALIDATION OF THE HOMOGENIZED MODEL

The developed homogenized material model is used to simulate response of a  $2.5\text{m} \times 2.5\text{m}$  unreinforced masonry (URM) wall with a concentrically positioned  $1200\text{ mm} \times 1000\text{ mm}$  opening under out-of-plane static loading with and without pre-compression  $0.1\text{ MPa}$  in vertical direction as shown in Figure 8. The same masonry wall is also analyzed with distinctive model in which brick and mortar materials in the model are discretized individually. The wall configurations and four side boundaries set-up in this experimental study are also illustrated in Figure 8. In these experimental tests, airbags were used to apply a uniformly distributed pressure only onto the solid portions of the wall. The load applied on the wall using the airbags was measured using load cells positioned between the airbag backing board and the reaction frame and the pressure acting on the wall surface was calculated by dividing the total load by the area of the wall. Linear variable differential transformers (LVDT) were used to measure displacements at different targets. Details about the experimental study can be found in another study (Griffith and Vaculik 2007). Figure 9 shows distinctive model and homogenized models of the masonry walls and the element numbers used for the distinctive model and the homogenized model are 319,854 and 3,988 respectively. The material models of mortar and brick as well as homogenized material model for masonry including the equivalent elastic properties, failure criteria are input into an available computer program LS-DYNA3D in an orthotropic composite damage model for analysis.

Figure 10 shows pressure-displacement relationship from tests and numerical simulation of the wall with and without pre-compression  $0.1\text{ MPa}$  at the target. As shown in Figure 10a, both the

homogenized model and distinctive model a give good prediction of the URM wall response without pre-compression as compared with those obtained by experimental tests. However with the same computer system the time spent for the distinctive model to solve the problem is 20 hours while only 4 minutes is taken for the simple homogenized model. Again, similar responses are observed from the both models in comparison with the test results with pre-compression 0.1 MPa as shown in Figure 10b.

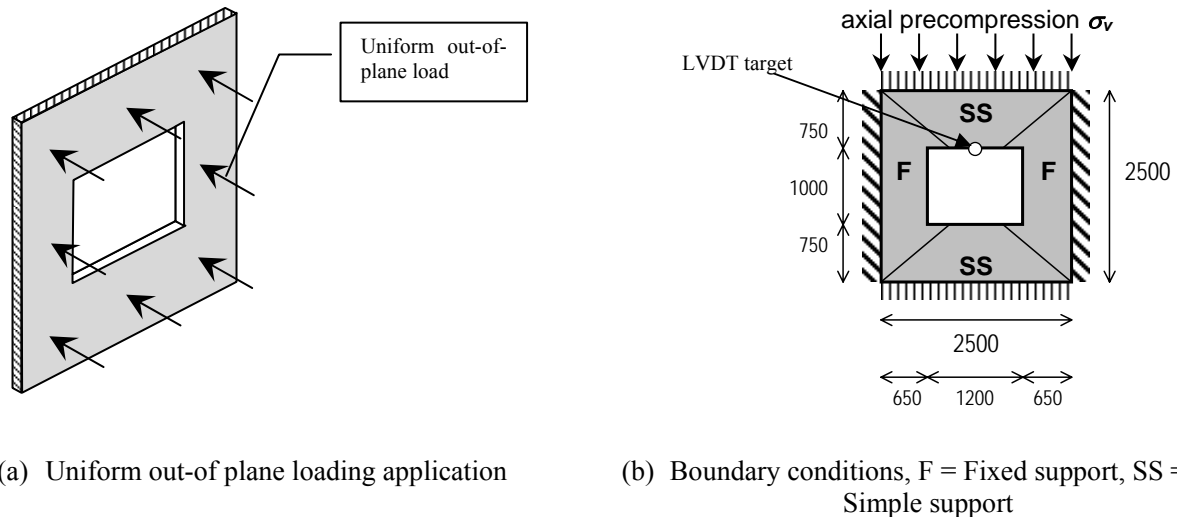


Figure 8 Configuration of URM wall with opening

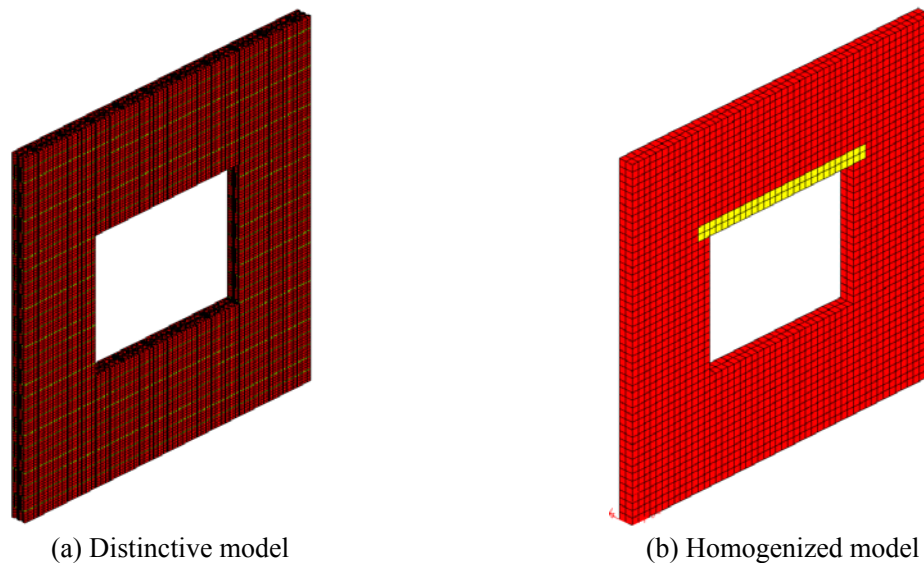


Fig. 9 Distinctive model and homogenized model of the URM walls wall opening

It should be noted that although the homogenized model gives reliable estimation of global response of URM wall to static loads with far less time compared with distinctive model, it may not yield accurate prediction of crack patterns of the URM wall as good as distinctive model

because the weak mortar joints may significantly affect the crack patterns. Figure 11 shows cracking patterns from tests with pre-compression 0.1 MPa in comparison with simulation of distinctive model. The shading in Figure 11 (b) indicates the displacement distribution normal to the plane of the wall. As shown the distinctive gives accurate prediction of the crack patterns. However, the homogenized model can not simulate crack patterns very well. Therefore for simulating local damage of URM walls, distinctive model is still very useful tool although it is very time consuming and computational ineffective.

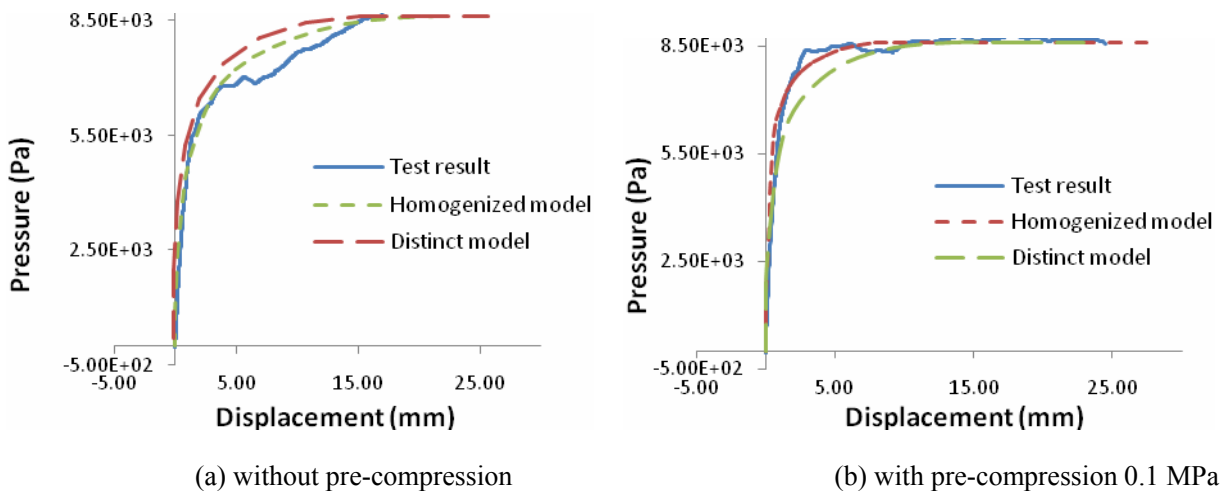


Figure 10 Comparison of results from the short wall with and without pre-compression test and simulation, (a) without pre-compression (b) URM wall with 0.1MPa pre-compression,

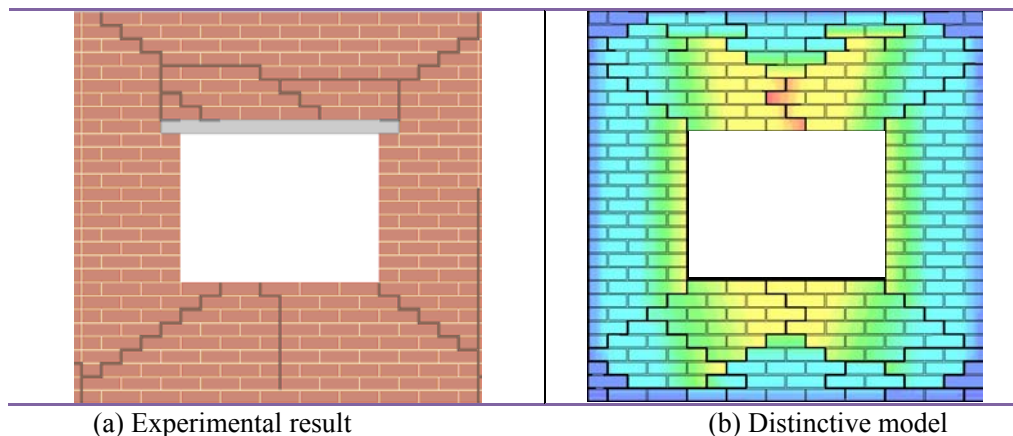


Figure 11 Cracking patterns from tests with pre-compression 0.1 MPa compared with simulation of distinctive model

## CONCLUSIONS

This paper presents numerical investigation of the ten-core brick URM wall using homogenization technique. The equivalent material properties of the masonry unit such as the elastic moduli and failure characteristics have been derived by numerical simulation of a basic

cell under various boundary conditions. The developed homogenized model is then used to simulate response of URM wall with opening under static loading. It was found that the simulated results using the homogenized model agree well with those obtained from distinctive model and test results. But, far less time is spent using the homogenized model in comparison with distinctive model. The developed homogenized model can be used to simulated large scale masonry structures under various loads. It is worth noting that although the homogenized model has demonstrated its computational efficiency to predict global response of the URM wall, it may not give good simulation of local damage such crack patterns of the URM wall in comparison of distinctive model.

## REFERENCES

- Anthoine A., “Derivation of the in-plane elastic characteristics of masonry through homogenization theory”, *International Journal of Solids and Structures*, 32 (2), 137-163, 1995.
- Griffith, MC and Vaculik, J, “Static tests of unreinforced brick masonry walls in 2-way bending,” *TMS Journal*, The Masonry Society, Boulder, Colorado, (accepted for publication 2007)
- Luciano R and Sacco E., “Homogenization technique and damage model for masonry material”, *International Journal of Solids and Structures*, 34 (24), 3191-3208, 1997.
- Ma GW, Hao H, Lu Y., “Homogenization of masonry using numerical simulation”, *Journal of Engineering Mechanics*, ASCE, Vol. 127 (5), 421-431, 2001.
- Milani G, Lourenco PB, Tralli A., “Homogenization approach for the limit analysis of out-of-plane loaded masonry walls”, *Journal of Structural Engineering*, ASCE, 130(10), 1650-1663, 2006.
- Wu C., Hao, H., “Numerical derivation of average material properties of hollow concrete block masonry”, *Engineering Structures*, 2007 (accepted).
- Zucchini A, Lourenco PB., “A micro-mechanical model for the homogenisation of masonry”, *International Journal of Solids and Structures*, 39 (12), 3233-3255, 2002.
- Zucchini A, Lourenco PB., “A coupled homogenisation-damage model for masonry cracking”, *Computers & Structures*, 82 (11-12), 917-929, 2004.